

Search for a heavy resonance decaying into a Z + jet final state in $p\bar{p}$ collisions at $\sqrt{s} = 1.96$ TeV using the D0 detector

V. M. Abazov,³⁶ B. Abbott,⁷⁶ M. Abolins,⁶⁶ B. S. Acharya,²⁹ M. Adams,⁵² T. Adams,⁵⁰ M. Agelou,¹⁸ J.-L. Agram,¹⁹ S. H. Ahn,³¹ M. Ahsan,⁶⁰ G. D. Alexeev,³⁶ G. Alkhalaf,⁴⁰ A. Alton,⁶⁵ G. Alverson,⁶⁴ G. A. Alves,² M. Anastasoae,³⁵ T. Andeen,⁵⁴ S. Anderson,⁴⁶ B. Andrieu,¹⁷ M. S. Anzelc,⁵⁴ Y. Arnaud,¹⁴ M. Arov,⁵³ A. Askew,⁵⁰ B. Åsman,⁴¹ A. C. S. Assis Jesus,³ O. Atramentov,⁵⁸ C. Autermann,²¹ C. Avila,⁸ C. Ay,²⁴ F. Badaud,¹³ A. Baden,⁶² L. Bagby,⁵³ B. Baldin,⁵¹ D. V. Bandurin,⁵⁹ P. Banerjee,²⁹ S. Banerjee,⁶⁴ E. Barberis,⁶⁴ P. Bargassa,⁸¹ P. Baringer,⁵⁹ C. Barnes,⁴⁴ J. Barreto,² J. F. Bartlett,⁵¹ U. Bassler,¹⁷ D. Bauer,⁴⁴ A. Bean,⁵⁹ M. Begalli,³ M. Begel,⁷² C. Belanger-Champagne,⁵ L. Bellantoni,⁵¹ A. Bellavance,⁶⁸ J. A. Benitez,⁶⁶ S. B. Beri,²⁷ G. Bernardi,¹⁷ R. Bernhard,⁴² L. Berntzon,¹⁵ I. Bertram,⁴³ M. Besançon,¹⁸ R. Beuselinck,⁴⁴ V. A. Bezzubov,³⁹ P. C. Bhat,⁵¹ V. Bhatnagar,²⁷ M. Binder,²⁵ C. Biscarat,⁴³ K. M. Black,⁶³ I. Blackler,⁴⁴ G. Blazey,⁵³ F. Blekman,⁴⁴ S. Blessing,⁵⁰ D. Bloch,¹⁹ K. Bloom,⁶⁸ U. Blumenschein,²³ A. Boehnlein,⁵¹ O. Boeriu,⁵⁶ T. A. Bolton,⁶⁰ F. Borchering,⁵¹ G. Borissov,⁴³ K. Bos,³⁴ T. Bose,⁷⁸ A. Brandt,⁷⁹ R. Brock,⁶⁶ G. Brooijmans,⁷¹ A. Bross,⁵¹ D. Brown,⁷⁹ N. J. Buchanan,⁵⁰ D. Buchholz,⁵⁴ M. Buehler,⁸² V. Buescher,²³ S. Burdin,⁵¹ S. Burke,⁴⁶ T. H. Burnett,⁸³ E. Busato,¹⁷ C. P. Buszello,⁴⁴ J. M. Butler,⁶³ P. Calfayan,²⁵ S. Calvet,¹⁵ J. Cammin,⁷² S. Caron,³⁴ W. Carvalho,³ B. C. K. Casey,⁷⁸ N. M. Cason,⁵⁶ H. Castilla-Valdez,³³ S. Chakrabarti,²⁹ D. Chakraborty,⁵³ K. M. Chan,⁷² A. Chandra,⁴⁹ D. Chapin,⁷⁸ F. Charles,¹⁹ E. Cheu,⁴⁶ F. Chevallier,¹⁴ D. K. Cho,⁶³ S. Choi,³² B. Choudhary,²⁸ L. Christofek,⁵⁹ D. Claes,⁶⁸ B. Clément,¹⁹ C. Clément,⁴¹ Y. Coadou,⁵ M. Cooke,⁸¹ W. E. Cooper,⁵¹ D. Coppage,⁵⁹ M. Corcoran,⁸¹ M.-C. Cousinou,¹⁵ B. Cox,⁴⁵ S. Crépe-Renaudin,¹⁴ D. Cutts,⁷⁸ M. Cwiok,³⁰ H. da Motta,² A. Das,⁶³ M. Das,⁶¹ B. Davies,⁴³ G. Davies,⁴⁴ G. A. Davis,⁵⁴ K. De,⁷⁹ P. de Jong,³⁴ S. J. de Jong,³⁵ E. De La Cruz-Burelo,⁶⁵ C. De Oliveira Martins,³ J. D. Degenhardt,⁶⁵ F. Déliot,¹⁸ M. Demarteau,⁵¹ R. Demina,⁷² P. Demine,¹⁸ D. Denisov,⁵¹ S. P. Denisov,³⁹ S. Desai,⁷³ H. T. Diehl,⁵¹ M. Diesburg,⁵¹ M. Doidge,⁴³ A. Dominguez,⁶⁸ H. Dong,⁷³ L. V. Dudko,³⁸ L. Duflot,¹⁶ S. R. Dugad,²⁹ A. Duperrin,¹⁵ J. Dyer,⁶⁶ A. Dyshkant,⁵³ M. Eads,⁶⁸ D. Edmunds,⁶⁶ T. Edwards,⁴⁵ J. Ellison,⁴⁹ J. Elmsheuser,²⁵ V. D. Elvira,⁵¹ S. Eno,⁶² P. Ermolov,³⁸ J. Estrada,⁵¹ H. Evans,⁵⁵ A. Evdokimov,³⁷ V. N. Evdokimov,³⁹ S. N. Fatakia,⁶³ L. Felgioni,⁶³ A. V. Ferapontov,⁶⁰ T. Ferbel,⁷² F. Fiedler,²⁵ F. Filthaut,³⁵ W. Fisher,⁵¹ H. E. Fisk,⁵¹ I. Fleck,²³ M. Ford,⁴⁵ M. Fortner,⁵³ H. Fox,²³ S. Fu,⁵¹ S. Fuess,⁵¹ T. Gadfort,⁸³ C. F. Galea,³⁵ E. Gallas,⁵¹ E. Galyaev,⁵⁶ C. Garcia,⁷² A. Garcia-Bellido,⁸³ J. Gardner,⁵⁹ V. Gavrilov,³⁷ A. Gay,¹⁹ P. Gay,¹³ D. Gelé,¹⁹ R. Gelhaus,⁴⁹ C. E. Gerber,⁵² Y. Gershtein,⁵⁰ D. Gillberg,⁵ G. Ginter,⁷² N. Gollub,⁴¹ B. Gómez,⁸ K. Gounder,⁵¹ A. Goussiou,⁵⁶ P. D. Grannis,⁷³ H. Greenlee,⁵¹ Z. D. Greenwood,⁶¹ E. M. Gregores,⁴ G. Grenier,²⁰ Ph. Gris,¹³ J.-F. Grivaz,¹⁶ S. Grünendahl,⁵¹ M. W. Grünewald,³⁰ F. Guo,⁷³ J. Guo,⁷³ G. Gutierrez,⁵¹ P. Gutierrez,⁷⁶ A. Haas,⁷¹ N. J. Hadley,⁶² P. Haefner,²⁵ S. Hagopian,⁵⁰ J. Haley,⁶⁹ I. Hall,⁷⁶ R. E. Hall,⁴⁸ L. Han,⁷ K. Hanagaki,⁵¹ K. Harder,⁶⁰ A. Harel,⁷² R. Harrington,⁶⁴ J. M. Hauptman,⁵⁸ R. Hauser,⁶⁶ J. Hays,⁵⁴ T. Hebbeker,²¹ D. Hedin,⁵³ J. G. Hegeman,³⁴ J. M. Heinmiller,⁵² A. P. Heinson,⁴⁹ U. Heintz,⁶³ C. Hensel,⁵⁹ G. Hesketh,⁶⁴ M. D. Hildreth,⁵⁶ R. Hirosky,⁸² J. D. Hobbs,⁷³ B. Hoeneisen,¹² H. Hoeth,²⁶ M. Hohlfeld,¹⁶ S. J. Hong,³¹ R. Hooper,⁷⁸ P. Houben,³⁴ Y. Hu,⁷³ Z. Hubacek,¹⁰ V. Hynek,⁹ I. Iashvili,⁷⁰ R. Illingworth,⁵¹ A. S. Ito,⁵¹ S. Jabeen,⁶³ M. Jaffré,¹⁶ S. Jain,⁷⁶ K. Jakobs,²³ C. Jarvis,⁶² A. Jenkins,⁴⁴ R. Jesik,⁴⁴ K. Johns,⁴⁶ C. Johnson,⁷¹ M. Johnson,⁵¹ A. Jonckheere,⁵¹ P. Jonsson,⁴⁴ A. Juste,⁵¹ D. Käfer,²¹ S. Kahn,⁷⁴ E. Kajfasz,¹⁵ A. M. Kalinin,³⁶ J. M. Kalk,⁶¹ J. R. Kalk,⁶⁶ S. Kappler,²¹ D. Karmanov,³⁸ J. Kasper,⁶³ P. Kasper,⁵¹ I. Katsanos,⁷¹ D. Kau,⁵⁰ R. Kaur,²⁷ R. Kehoe,⁸⁰ S. Kermiche,¹⁵ S. Kesisoglou,⁷⁸ N. Khalatyan,⁶³ A. Khanov,⁷⁷ A. Kharchilava,⁷⁰ Y. M. Kharzheev,³⁶ D. Khatidze,⁷¹ H. Kim,⁷⁹ T. J. Kim,³¹ M. H. Kirby,³⁵ B. Klima,⁵¹ J. M. Kohli,²⁷ J.-P. Konrath,²³ M. Kopal,⁷⁶ V. M. Korablev,³⁹ J. Kotcher,⁷⁴ B. Kothari,⁷¹ A. Koubarovsky,³⁸ A. V. Kozelov,³⁹ J. Kozminski,⁶⁶ A. Kryemadhi,⁸² S. Krzywdzinski,⁵¹ T. Kuhl,²⁴ A. Kumar,⁷⁰ S. Kunori,⁶² A. Kupco,¹¹ T. Kurča,^{20,*} J. Kvita,⁹ S. Lager,⁴¹ S. Lammers,⁷¹ G. Landsberg,⁷⁸ J. Lazoflores,⁵⁰ A.-C. Le Bihan,¹⁹ P. Lebrun,²⁰ W. M. Lee,⁵³ A. Leflat,³⁸ F. Lehner,⁴² V. Lesne,¹³ J. Leveque,⁴⁶ P. Lewis,⁴⁴ J. Li,⁷⁹ Q. Z. Li,⁵¹ J. G. R. Lima,⁵³ D. Lincoln,⁵¹ J. Linnemann,⁶⁶ V. V. Lipaev,³⁹ R. Lipton,⁵¹ Z. Liu,⁵ L. Lobo,⁴⁴ A. Lobodenko,⁴⁰ M. Lokajicek,¹¹ A. Lounis,¹⁹ P. Love,⁴³ H. J. Lubatti,⁸³ M. Lynker,⁵⁶ A. L. Lyon,⁵¹ A. K. A. Maciel,² R. J. Madaras,⁴⁷ P. Mättig,²⁶ C. Magass,²¹ A. Magerkurth,⁶⁵ A.-M. Magnan,¹⁴ N. Makovec,¹⁶ P. K. Mal,⁵⁶ H. B. Malbouisson,³ S. Malik,⁶⁸ V. L. Malyshev,³⁶ H. S. Mao,⁶ Y. Maravin,⁶⁰ M. Martens,⁵¹ S. E. K. Mattingly,⁷⁸ R. McCarthy,⁷³ R. McCroskey,⁴⁶ D. Meder,²⁴ A. Melnitchouk,⁶⁷ A. Mendes,¹⁵ L. Mendoza,⁸ M. Merkin,³⁸ K. W. Merritt,⁵¹ A. Meyer,²¹ J. Meyer,²² M. Michaut,¹⁸ H. Miettinen,⁸¹ T. Millet,²⁰ J. Mitrevski,⁷¹ J. Molina,³ N. K. Mondal,²⁹ J. Monk,⁴⁵ R. W. Moore,⁵ T. Moulik,⁵⁹ G. S. Muanza,¹⁶ M. Mulders,⁵¹ M. Mulhearn,⁷¹ L. Mundim,³ Y. D. Mutaf,⁷³ E. Nagy,¹⁵ M. Naimuddin,²⁸ M. Narain,⁶³ N. A. Naumann,³⁵ H. A. Neal,⁶⁵ J. P. Negret,⁸ S. Nelson,⁵⁰ P. Neustroev,⁴⁰ C. Noeding,²³ A. Nomerotski,⁵¹ S. F. Novaes,⁴ T. Nunnemann,²⁵ V. O'Dell,⁵¹ D. C. O'Neil,⁵ G. Obrant,⁴⁰ V. Oguri,³ N. Oliveira,³

N. Oshima,⁵¹ R. Otec,¹⁰ G. J. Otero y Garzón,⁵² M. Owen,⁴⁵ P. Padley,⁸¹ N. Parashar,⁵⁷ S.-J. Park,⁷² S. K. Park,³¹ J. Parsons,⁷¹ R. Partridge,⁷⁸ N. Parua,⁷³ A. Patwa,⁷⁴ G. Pawloski,⁸¹ P. M. Perea,⁴⁹ E. Perez,¹⁸ K. Peters,⁴⁵ P. Pétrouff,¹⁶ M. Petteni,⁴⁴ R. Piegaia,¹ M.-A. Pleier,²² P. L. M. Podesta-Lerma,³³ V. M. Podstavkov,⁵¹ Y. Pogorelov,⁵⁶ M.-E. Pol,² A. Pompos,⁷⁶ B. G. Pope,⁶⁶ A. V. Popov,³⁹ W. L. Prado da Silva,³ H. B. Prosper,⁵⁰ S. Protopopescu,⁷⁴ J. Qian,⁶⁵ A. Quadt,²² B. Quinn,⁶⁷ K. J. Rani,²⁹ K. Ranjan,²⁸ P. A. Rapidis,⁵¹ P. N. Ratoff,⁴³ P. Renkel,⁸⁰ S. Reucroft,⁶⁴ M. Rijssenbeek,⁷³ I. Ripp-Baudot,¹⁹ F. Rizatdinova,⁷⁷ S. Robinson,⁴⁴ R. F. Rodrigues,³ C. Royon,¹⁸ P. Rubinov,⁵¹ R. Ruchti,⁵⁶ V. I. Rud,³⁸ G. Sajot,¹⁴ A. Sánchez-Hernández,³³ M. P. Sanders,⁶² A. Santoro,³ G. Savage,⁵¹ L. Sawyer,⁶¹ T. Scanlon,⁴⁴ D. Schaile,²⁵ R. D. Schamberger,⁷³ Y. Scheglov,⁴⁰ H. Schellman,⁵⁴ P. Schieferdecker,²⁵ C. Schmitt,²⁶ C. Schwanenberger,⁴⁵ A. Schwartzman,⁶⁹ R. Schwienhorst,⁶⁶ S. Sengupta,⁵⁰ H. Severini,⁷⁶ E. Shabalina,⁵² M. Shamim,⁶⁰ V. Shary,¹⁸ A. A. Shchukin,³⁹ W. D. Shephard,⁵⁶ R. K. Shivpuri,²⁸ D. Shpakov,⁶⁴ V. Siccaldi,¹⁹ R. A. Sidwell,⁶⁰ V. Simak,¹⁰ V. Sirotenko,⁵¹ P. Skubic,⁷⁶ P. Slattery,⁷² R. P. Smith,⁵¹ G. R. Snow,⁶⁸ J. Snow,⁷⁵ S. Snyder,⁷⁴ S. Söldner-Rembold,⁴⁵ X. Song,⁵³ L. Sonnenschein,¹⁷ A. Sopczak,⁴³ M. Sosebee,⁷⁹ K. Soustruznik,⁹ M. Souza,² B. Spurlock,⁷⁹ J. Stark,¹⁴ J. Steele,⁶¹ K. Stevenson,⁵⁵ V. Stolin,³⁷ A. Stone,⁵² D. A. Stoyanova,³⁹ J. Strandberg,⁴¹ M. A. Strang,⁷⁰ M. Strauss,⁷⁶ R. Ströhmer,²⁵ D. Strom,⁵⁴ M. Strovink,⁴⁷ L. Stutte,⁵¹ S. Sumowidagdo,⁵⁰ A. Sznajder,³ M. Talby,¹⁵ P. Tamburello,⁴⁶ W. Taylor,⁵ P. Telford,⁴⁵ J. Temple,⁴⁶ E. Thomas,¹⁵ B. Tiller,²⁵ M. Titov,²³ V. V. Tokmenin,³⁶ M. Tomoto,⁵¹ T. Toole,⁶² I. Torchiani,²³ S. Towers,⁴³ T. Trefzger,²⁴ S. Trincaz-Duvoid,¹⁷ D. Tsybychev,⁷³ B. Tuchming,¹⁸ C. Tully,⁶⁹ A. S. Turcot,⁴⁵ P. M. Tuts,⁷¹ R. Unalan,⁶⁶ L. Uvarov,⁴⁰ S. Uvarov,⁴⁰ S. Uzunyan,⁵³ B. Vachon,⁵ P. J. van den Berg,³⁴ R. Van Kooten,⁵⁵ W. M. van Leeuwen,³⁴ N. Varelas,⁵² E. W. Varnes,⁴⁶ A. Vartapetian,⁷⁹ I. A. Vasilyev,³⁹ M. Vaupel,²⁶ P. Verdier,²⁰ L. S. Vertogradov,³⁶ M. Verzocchi,⁵¹ F. Villeneuve-Segulier,⁴⁴ P. Vint,⁴⁴ J.-R. Vlimant,¹⁷ E. Von Toerne,⁶⁰ M. Voutilainen,^{68,†} M. Vreeswijk,³⁴ H. D. Wahl,⁵⁰ L. Wang,⁶² J. Warchol,⁵⁶ G. Watts,⁸³ M. Wayne,⁵⁶ M. Weber,⁵¹ H. Weerts,⁶⁶ N. Wermes,²² M. Wetstein,⁶² A. White,⁷⁹ D. Wicke,²⁶ G. W. Wilson,⁵⁹ S. J. Wimpenny,⁴⁹ M. Wobisch,⁵¹ J. Womersley,⁵¹ D. R. Wood,⁶⁴ T. R. Wyatt,⁴⁵ Y. Xie,⁷⁸ N. Xuan,⁵⁶ S. Yacoub,⁵⁴ R. Yamada,⁵¹ M. Yan,⁶² T. Yasuda,⁵¹ Y. A. Yatsunenko,³⁶ K. Yip,⁷⁴ H. D. Yoo,⁷⁸ S. W. Youn,⁵⁴ C. Yu,¹⁴ J. Yu,⁷⁹ A. Yurkewicz,⁷³ A. Zatserklyaniy,⁵³ C. Zeitnitz,²⁶ D. Zhang,⁵¹ T. Zhao,⁸³ Z. Zhao,⁶⁵ B. Zhou,⁶⁵ J. Zhu,⁷³ M. Zielinski,⁷² D. Zieminska,⁵⁵ A. Zieminski,⁵⁵ V. Zutshi,⁵³ and E. G. Zverev³⁸

(D0 Collaboration)

¹Universidad de Buenos Aires, Buenos Aires, Argentina

²LAFEX, Centro Brasileiro de Pesquisas Físicas, Rio de Janeiro, Brazil

³Universidade do Estado do Rio de Janeiro, Rio de Janeiro, Brazil

⁴Instituto de Física Teórica, Universidade Estadual Paulista, São Paulo, Brazil

⁵University of Alberta, Edmonton, Alberta, Canada, Simon Fraser University, Burnaby, British Columbia, Canada, York University, Toronto, Ontario, Canada, and McGill University, Montreal, Quebec, Canada

⁶Institute of High Energy Physics, Beijing, People's Republic of China

⁷University of Science and Technology of China, Hefei, People's Republic of China

⁸Universidad de los Andes, Bogotá, Colombia

⁹Center for Particle Physics, Charles University, Prague, Czech Republic

¹⁰Czech Technical University, Prague, Czech Republic

¹¹Center for Particle Physics, Institute of Physics, Academy of Sciences of the Czech Republic, Prague, Czech Republic

¹²Universidad San Francisco de Quito, Quito, Ecuador

¹³Laboratoire de Physique Corpusculaire, IN2P3-CNRS, Université Blaise Pascal, Clermont-Ferrand, France

¹⁴Laboratoire de Physique Subatomique et de Cosmologie, IN2P3-CNRS, Université de Grenoble I, Grenoble, France

¹⁵CPPM, IN2P3-CNRS, Université de la Méditerranée, Marseille, France

¹⁶IN2P3-CNRS, Laboratoire de l'Accélérateur Linéaire, Orsay, France

¹⁷LPNHE, IN2P3-CNRS, Universités Paris VI and VII, Paris, France

¹⁸DAPNIA/Service de Physique des Particules, CEA, Saclay, France

¹⁹IReS, IN2P3-CNRS, Université Louis Pasteur, Strasbourg, France, and Université de Haute Alsace, Mulhouse, France

²⁰Institut de Physique Nucléaire de Lyon, IN2P3-CNRS, Université Claude Bernard, Villeurbanne, France

²¹III. Physikalisches Institut A, RWTH Aachen, Aachen, Germany

²²Physikalisches Institut, Universität Bonn, Bonn, Germany

²³Physikalisches Institut, Universität Freiburg, Freiburg, Germany

²⁴Institut für Physik, Universität Mainz, Mainz, Germany

²⁵Ludwig-Maximilians-Universität München, München, Germany

²⁶Fachbereich Physik, University of Wuppertal, Wuppertal, Germany

²⁷Panjab University, Chandigarh, India

- ²⁸Delhi University, Delhi, India
²⁹Tata Institute of Fundamental Research, Mumbai, India
³⁰University College Dublin, Dublin, Ireland
³¹Korea Detector Laboratory, Korea University, Seoul, Korea
³²SungKyunKwan University, Suwon, Korea
³³CINVESTAV, Mexico City, Mexico
³⁴FOM-Institute NIKHEF and University of Amsterdam/NIKHEF, Amsterdam, The Netherlands
³⁵Radboud University Nijmegen/NIKHEF, Nijmegen, The Netherlands
³⁶Joint Institute for Nuclear Research, Dubna, Russia
³⁷Institute for Theoretical and Experimental Physics, Moscow, Russia
³⁸Moscow State University, Moscow, Russia
³⁹Institute for High Energy Physics, Protvino, Russia
⁴⁰Petersburg Nuclear Physics Institute, St. Petersburg, Russia
⁴¹Lund University, Lund, Sweden, Royal Institute of Technology and Stockholm University, Stockholm, Sweden, and Uppsala University, Uppsala, Sweden
⁴²Physik Institut der Universität Zürich, Zürich, Switzerland
⁴³Lancaster University, Lancaster, United Kingdom
⁴⁴Imperial College, London, United Kingdom
⁴⁵University of Manchester, Manchester, United Kingdom
⁴⁶University of Arizona, Tucson, Arizona 85721, USA
⁴⁷Lawrence Berkeley National Laboratory and University of California, Berkeley, California 94720, USA
⁴⁸California State University, Fresno, California 93740, USA
⁴⁹University of California, Riverside, California 92521, USA
⁵⁰Florida State University, Tallahassee, Florida 32306, USA
⁵¹Fermi National Accelerator Laboratory, Batavia, Illinois 60510, USA
⁵²University of Illinois at Chicago, Chicago, Illinois 60607, USA
⁵³Northern Illinois University, DeKalb, Illinois 60115, USA
⁵⁴Northwestern University, Evanston, Illinois 60208, USA
⁵⁵Indiana University, Bloomington, Indiana 47405, USA
⁵⁶University of Notre Dame, Notre Dame, Indiana 46556, USA
⁵⁷Purdue University Calumet, Hammond, Indiana 46323, USA
⁵⁸Iowa State University, Ames, Iowa 50011, USA
⁵⁹University of Kansas, Lawrence, Kansas 66045, USA
⁶⁰Kansas State University, Manhattan, Kansas 66506, USA
⁶¹Louisiana Tech University, Ruston, Louisiana 71272, USA
⁶²University of Maryland, College Park, Maryland 20742, USA
⁶³Boston University, Boston, Massachusetts 02215, USA
⁶⁴Northeastern University, Boston, Massachusetts 02115, USA
⁶⁵University of Michigan, Ann Arbor, Michigan 48109, USA
⁶⁶Michigan State University, East Lansing, Michigan 48824, USA
⁶⁷University of Mississippi, University, Mississippi 38677, USA
⁶⁸University of Nebraska, Lincoln, Nebraska 68588, USA
⁶⁹Princeton University, Princeton, New Jersey 08544, USA
⁷⁰State University of New York, Buffalo, New York 14260, USA
⁷¹Columbia University, New York, New York 10027, USA
⁷²University of Rochester, Rochester, New York 14627, USA
⁷³State University of New York, Stony Brook, New York 11794, USA
⁷⁴Brookhaven National Laboratory, Upton, New York 11973, USA
⁷⁵Langston University, Langston, Oklahoma 73050, USA
⁷⁶University of Oklahoma, Norman, Oklahoma 73019, USA
⁷⁷Oklahoma State University, Stillwater, Oklahoma 74078, USA
⁷⁸Brown University, Providence, Rhode Island 02912, USA
⁷⁹University of Texas, Arlington, Texas 76019, USA
⁸⁰Southern Methodist University, Dallas, Texas 75275, USA
⁸¹Rice University, Houston, Texas 77005, USA
⁸²University of Virginia, Charlottesville, Virginia 22901, USA
⁸³University of Washington, Seattle, Washington 98195, USA

*On leave from IEP SAS Kosice, Slovakia.

†Visitor from Helsinki Institute of Physics, Helsinki, Finland.

(Received 9 June 2006; published 17 July 2006)

We have searched for a heavy resonance decaying into a $Z + \text{jet}$ final state in $p\bar{p}$ collisions at a center of mass energy of 1.96 TeV at the Fermilab Tevatron collider using the D0 detector. No indication for such a resonance was found in a data sample corresponding to an integrated luminosity of 370 pb^{-1} . We set upper limits on the cross section times branching fraction for heavy resonance production at the 95% C.L. as a function of the resonance mass and width. The limits are interpreted within the framework of a specific model of excited quark production.

DOI: [10.1103/PhysRevD.74.011104](https://doi.org/10.1103/PhysRevD.74.011104)

PACS numbers: 13.85.Rm, 14.65.-q, 14.70.Hp, 14.80.-j

Heavy resonances decaying into a quark and a gauge boson may signal the existence of excited quarks and thereby indicate quark substructure [1]. Searches for excited quarks have been carried out in the past using dijet [2–4], photon + jet, and $W + \text{jet}$ [5] final states. In the analysis described here, we searched for resonances in the $Z + \text{jet}$ channel, where the Z boson is detected via its $Z \rightarrow e^+e^-$ decay mode. This signature is practically free of instrumental background. However, it suffers from the low branching fraction (3.36%) of the $Z \rightarrow e^+e^-$ decay channel. The high luminosity delivered by the Fermilab Tevatron collider in Run II makes it possible to present results on this final state for the first time.

For the production and decay of a resonance, we considered the model [1] implemented in PYTHIA 6.202 [6]. Here, a quark (antiquark) and a gluon from the colliding proton and antiproton form a resonance, q^* , which subsequently decays into a Z boson and a quark: $q^* \rightarrow q + Z$. The model has two free parameters, M_{q^*} , the mass of the resonance, and Λ , the compositeness scale which determine the production cross section and the natural width of the resonance. The latter scales as $1/\xi^2$, where $\xi = \Lambda/M_{q^*}$.

The Run II D0 detector [7] consists of several layered subdetectors. For the present analysis, the most relevant parts are the liquid-argon/uranium calorimeter [8] and the central tracking system. The calorimeter, divided into electromagnetic and hadronic sections, has a granularity of $\Delta\eta \times \Delta\phi = 0.1 \times 0.1$, where η is the pseudorapidity ($\eta = -\ln[\tan(\theta/2)]$ with θ being the polar angle measured from the geometrical center of the detector with respect to the proton beam direction) and ϕ is the azimuthal angle. The third innermost layer, in which the largest electromagnetic energy deposition is expected, has a finer granularity of $\Delta\eta \times \Delta\phi = 0.05 \times 0.05$. The central calorimeter covers $|\eta| \leq 1.1$, and the two end calorimeters extend coverage to $|\eta| \approx 4.5$. The tracking system consists of a silicon microstrip tracker and a central fiber tracker, both located within a 2 T superconducting solenoidal magnet, with designs optimized for tracking and vertexing at pseudorapidities $|\eta| < 3$ and $|\eta| < 2$, respectively.

The data used in this analysis were collected between April 2002 and August 2004, with an integrated luminosity of 370 pb^{-1} . The selected events were required to pass at least one of several single- or di-electron triggers. The

efficiency of the trigger was measured with data and found to reach a plateau of $\varepsilon_{\text{trig}} = 0.982 \pm 0.011$ for events satisfying the final event selection criteria.

Offline event selection was based on run quality, event properties, and electron and jet identification criteria. Events were required to have a reconstructed vertex with a longitudinal position within 60 cm of the detector center. Electrons were reconstructed from electromagnetic (EM) clusters in the calorimeter using a cone algorithm. The reconstructed electron candidates were required to satisfy either $|\eta| \leq 1.1$ or $1.5 < |\eta| \leq 2.5$. Electron pairs with $p_T^{e1} \geq 30 \text{ GeV}$ and $p_T^{e2} \geq 25 \text{ GeV}$ in the event were used to reconstruct the Z boson candidate. The electron pair was required to have an invariant mass M_{ee} in the region $80 < M_{ee} < 102 \text{ GeV}$ near the Z boson mass of 91.2 GeV.

To reduce background contamination, mainly from jets misidentified as electrons, the EM clusters were required to pass three quality criteria based on shower profile: (i) the ratio of the energy deposited in the electromagnetic part of the calorimeter to the total shower energy had to exceed 0.9; (ii) the lateral and longitudinal shapes of the energy cluster had to be consistent with those of an electron; and (iii) the electron had to be isolated from other energy deposits in the calorimeter with isolation fraction $f_{\text{iso}} < 0.15$. The isolation fraction is defined as $f_{\text{iso}} = [E(0.4) - E_{\text{EM}}(0.2)]/E_{\text{EM}}(0.2)$, where $E(R_{\text{cone}})$ and $E_{\text{EM}}(R_{\text{cone}})$ are the total and the EM energy, respectively, deposited within a cone of radius $R_{\text{cone}} = \sqrt{(\Delta\eta)^2 + (\Delta\phi)^2}$ centered around the electron. Additionally, at least one of the electrons was required to have a spatially close track with a momentum consistent with the EM shower energy. A total of 24 734 events passed these criteria. In Fig. 1, the distribution of the invariant mass, M_{ee} , of the two selected electrons is shown. A very clean, almost background-free Z boson signal is evident.

Jets were reconstructed using the ‘‘Run II cone algorithm’’ [9] which combines cell energies within a cone of radius $R_{\text{cone}} = 0.5$. Spurious jets from isolated noisy calorimeter cells were suppressed by cuts on the jet shape and by requiring that the charged tracks associated with the jet had to carry a minimum fraction of the jet transverse energy. The transverse momentum of each jet was corrected for offsets due to the underlying event, multiple $p\bar{p}$ interactions and noise, out-of-cone showering, and the detector energy response as determined from the transverse

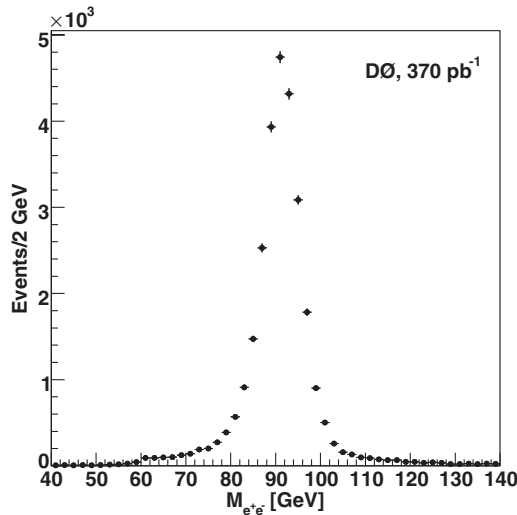


FIG. 1. The invariant mass of the two selected electrons in the data events.

energy balance of photon + jet events. Jets were required to have $p_T > 20$ GeV and $|\eta| < 2.5$ and to not overlap with any of the reconstructed EM objects within a distance of 0.4 in (η, ϕ) space. Requiring one or more jets with these selection criteria yielded a sample of 2417 events.

We have considered two kinds of instrumental backgrounds where hadronic jets are misreconstructed as EM clusters and mimic Z boson events. A background from genuine QCD multijet production arises when both of the EM objects are hadronic jets that fluctuate to electromagnetic final states. This background has been estimated to be $(0.56 \pm 0.02)\%$ of the signal in the mass region of $80 < M_{ee} < 102$ GeV as calculated by comparing the M_{ee} mass distribution of the selected events with a distribution where the lateral and longitudinal shapes of the energy clusters were not consistent with those of an electron and there was no track matching to these clusters. The other source of background is $W \rightarrow e\nu + \text{jets}$ events where a hadronic jet is misidentified as an electron. These events are characterized by significant missing transverse energy (\cancel{E}_T), and should also appear in the data sample where only one of

the EM objects has a matched track. From comparison of the \cancel{E}_T distribution of these events with that where both electrons do have matched tracks, we estimate that this background is an order of magnitude less than the QCD background.

The main standard model (SM) background to the excited quark signal is inclusive $Z/\gamma^* \rightarrow e^+e^-$ pair production. This process has been simulated with PYTHIA using the CTEQ5L [10] parton distribution functions (PDFs). In order to enhance the statistics for events where the invariant mass of the Z boson and the leading jet, M_{Zj1} , is high, in addition to the so-called $2 \rightarrow 1$ process, where the initial quark and antiquark annihilates into a Z boson, we have also generated events including matrix elements of first order in α_s ($2 \rightarrow 2$ process) where the produced Z boson is accompanied by a quark or a gluon in the final state. The threshold of M_{Zq} , the invariant mass of the Z boson and the accompanying parton, has been varied. A minimum value of 30 GeV for p_{Tp} , the transverse momentum of the parton in the $2 \rightarrow 2$ collision, has been set in order to avoid collinear divergences. The leading jet p_T distribution has a mean and an RMS value of 106 GeV and 27 GeV, respectively, at the lowest resonance mass investigated and after the final selection, therefore the p_{Tp} cut does not affect the analysis. The shape of the M_{Zj1} distribution has been compared with that obtained with the ALPGEN program [11] and there is reasonable agreement between them. Any differences in the background level have been taken into account as a systematic uncertainty.

Signal events were generated with PYTHIA using the CTEQ5L PDFs for the following resonance mass values: $M_{q^*} = 300, 400, 500, 600$ and 700 GeV with $\xi = \Lambda/M_{q^*} = 1$. For each mass, except for the lowest one, we also generated events with $\xi = 0.3, 0.5$ and 0.7 , in order to vary the natural width of the resonance, Γ_{q^*} . The form factors associated with the interaction of the quarks with the SM gauge bosons were set to unity. The MC events were passed through the same reconstruction software and selection criteria as the data. The events have been used to estimate the geometrical acceptance and jet and electron identification efficiencies. The combined ac-

TABLE I. Measured (σ_{95}) and expected (σ_{95}^{ave}) values of the upper limit on the resonance cross section times branching fraction, signal acceptance \times efficiency, SM background, and number of observed events at the optimal value of the topological cut k for different resonance masses and for $\xi = 1$.

M_{q^*} (GeV)	k	σ_{95} (pb)	σ_{95}^{ave} (pb)	Acceptance \times efficiency	SM background	Data (events)
300	1.1	0.25	0.290	0.140 ± 0.009	32.8 ± 2.9	31
400	1.2	0.15	0.129	0.164 ± 0.010	7.5 ± 0.8	9
500	1.3	0.08	0.079	0.195 ± 0.012	2.9 ± 0.8	3
600	1.8	0.05	0.053	0.244 ± 0.014	1.6 ± 0.6	1
700	1.7	0.03	0.044	0.243 ± 0.014	0.64 ± 0.06	0

ceptance times efficiencies are listed in Table I. The resolution of M_{Zj1} has been found to be $\approx 9\%$.

In Fig. 2 we compare the M_{Zj1} distribution of the data with the PYTHIA $2 \rightarrow 1$ process and with the PYTHIA $2 \rightarrow 2$ processes with various M_{Zq} thresholds. For the $2 \rightarrow 1$ process, the MC is normalized to the total number of data events. A different but common normalization factor is used for all $2 \rightarrow 2$ processes determined using the $M_{Zq} > 100$ GeV MC sample for $M_{Zj1} > 150$ GeV. The $2 \rightarrow 1$ simulation agrees well with the data but provides sufficient statistics only for $M_{Zj1} < 300$ GeV. On the other hand, the $2 \rightarrow 2$ processes describe the data with reasonable precision for $M_{Zj1} > 150$ GeV. Since the latter is the region of interest for the present search, we have used only the $2 \rightarrow 2$ process for estimation of the SM background with an M_{Zq} threshold chosen according to the M_{Zj1} region to be investigated. Also shown in Fig. 2 is the signal due to an excited quark of 500 GeV mass and narrow width ($\xi = 1$).

Since no significant excess of events is observed, which would indicate the presence of a resonance, we determined the upper limit on the production cross section of a hypothetical resonance as a function of its mass and width. We made use of the fact that in the p_{TZ} vs M_{Zj1} plane, events

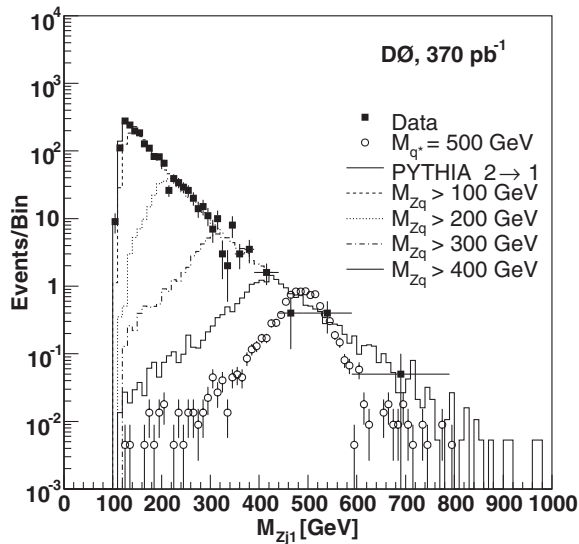


FIG. 2. Invariant mass distribution of the Z boson and the leading jet, M_{Zj1} . The data are shown by the full squares with error bars. The actual number of events in a bin is the product of the plotted value and the bin width measured in 10 GeV units. The SM backgrounds generated with PYTHIA are shown in the histograms: $2 \rightarrow 1$ without threshold (solid line), $2 \rightarrow 2$ with various M_{Zq} thresholds (discontinuous lines, as indicated). Each curve with a definite M_{Zq} threshold value stops when the curve of the next threshold value takes over. Also shown with open circles is the signal due to an excited quark of 500 GeV mass and narrow width ($\xi = 1$). The resonance production cross section is taken from Ref. [1].

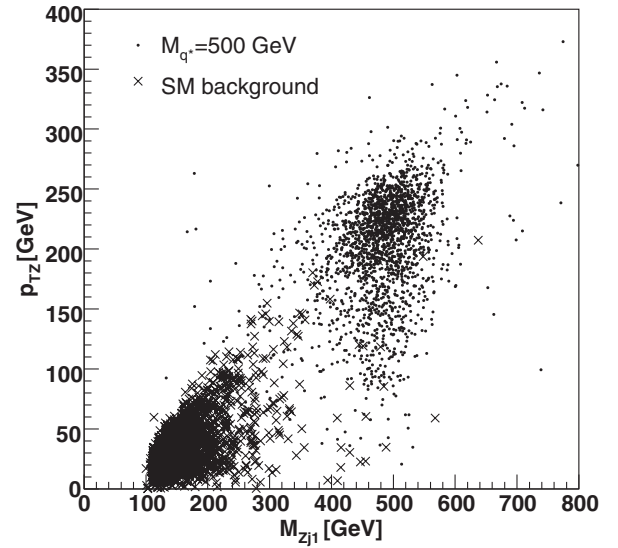


FIG. 3. p_{TZ} vs M_{Zj1} distributions for a resonance of mass of 500 GeV with $\xi = 1$ (dots) and for the SM background (crosses). Both the signal and background events passed through complete reconstruction. Each distribution is arbitrarily normalized.

from the resonance are concentrated for M_{Zj1} around the mass value and for p_{TZ} at about half of the mass value of the resonance, since the resonance is nearly at rest. The SM background does not exhibit a similar structure, as it is shown in Fig. 3. In addition, finite width and mass resolutions wash out the correlation between p_{TZ} and M_{Zj1} . We therefore considered events around the peak values M_{Zj1}^c and p_{TZ}^c of the resonance determined by the following condition:

$$\left(\frac{M_{Zj1} - M_{Zj1}^c}{M_{Zj1}^{\text{rms}}}\right)^2 + \left(\frac{p_{TZ} - p_{TZ}^c}{p_{TZ}^{\text{rms}}}\right)^2 < k^2 \quad (1)$$

and we optimized the cut value k . Here, M_{Zj1}^{rms} and p_{TZ}^{rms} are the RMS values of the corresponding distributions of the resonance. At given values of mass and width, the latter defined by ξ , we varied k in Eqn. (1) between 0 and 3 in steps of 0.1.

Based only on the information from the signal and background simulation, for each k we calculated σ_{95}^{ave} , the *expected value* of the upper limit on the resonance production cross section times branching fraction at the 95% C.L. using a Bayesian approach [12] and by averaging over possible outcomes of the background-only hypothesis assuming Poisson statistics for the background. The optimum value of k corresponds to the minimum value of σ_{95}^{ave} . At this value of k , using also the data, we derived σ_{95} , the *measured value* of the upper limit on the resonance production cross section times branching fraction at the 95%

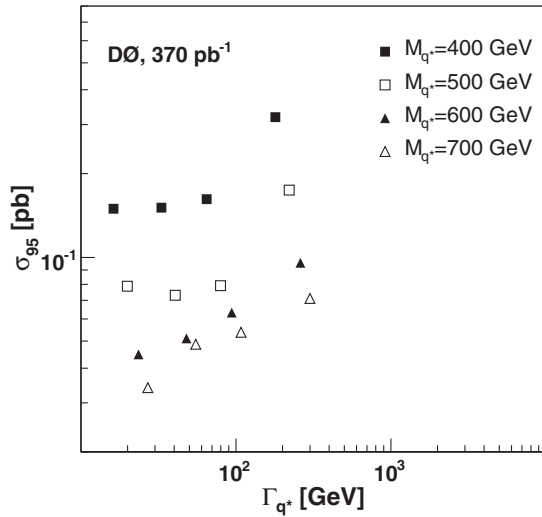


FIG. 4. Upper limit on the resonance cross section times branching fraction at the 95% C.L., σ_{95} , for different resonance masses as a function of the resonance width.

C.L. In this calculation we have taken into account systematic uncertainties in the determination of the luminosity (6.5%), trigger and identification efficiencies, and those of the jet calibration and resolution. Systematic uncertainties due to the modeling of the SM background and to the choice of the PDF, as well as those due to the threshold of the $M_{Zj1} > 150$ GeV in the normalization of the background, have also been included.

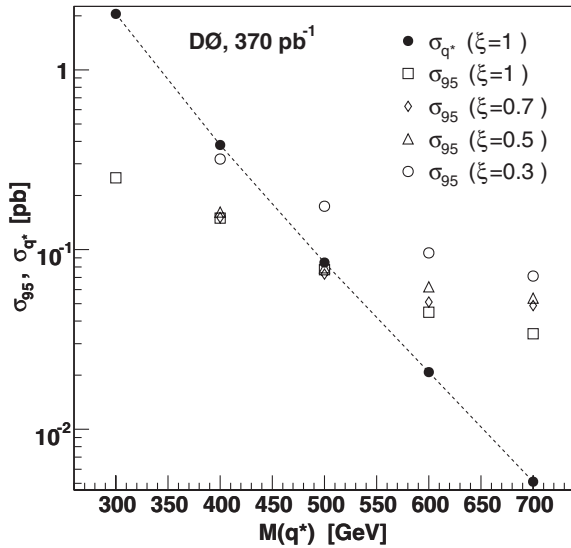


FIG. 5. Upper limits on the resonance cross section times branching fraction at the 95% C.L., σ_{95} , for different ξ values as functions of the resonance mass (open symbols). Full circles indicate the LO production cross section of an excited quark times its decay branching fraction into $Z + \text{jet}$ and $Z \rightarrow e^+e^-$, σ_{q^*} , for $\xi = 1$ [1].

TABLE II. Measured upper limit on the resonance cross section times branching fraction at the 95% C.L., σ_{95} , for different resonance masses and ξ values. σ_{q^*} , the production cross section of an excited quark times its decay branching fraction into $Z + \text{jet}$ and $Z \rightarrow e^+e^-$, is calculated in LO. The width for $\xi = 1$ is also shown [3] for each resonance mass. Cross sections are quoted in pb, whereas masses and widths are in GeV.

Mass	σ_{95}				σ_{q^*} $\xi = 1$	Γ_{q^*}
	$\xi = 0.3$	0.5	0.7	1		
300				0.25	2.045	13
400	0.32	0.16	0.15	0.15	0.382	16
500	0.17	0.08	0.07	0.08	0.084	20
600	0.10	0.06	0.05	0.05	0.021	24
700	0.07	0.05	0.05	0.03	0.005	27

In Table I, σ_{95} and σ_{95}^{ave} are shown together with the signal acceptance, the SM background level, and the number of data events for $\xi = 1$. The measured σ_{95} values are displayed in Fig. 4 and 5, and are compiled in Table II for different masses and widths (ξ). In Fig. 5, also shown is σ_{q^*} , the LO production cross section of an excited quark times its decay branching fraction into $Z + \text{jet}$ and $Z \rightarrow e^+e^-$, for $\xi = 1$ [1]. We find a lower limit of 510 GeV at the 95% C.L. for the mass of an excited quark for $\xi = 1$ within the framework of the model considered. In earlier measurements, lower bounds of 460, 530 and 775 GeV were obtained for the same quantity, but in different decay modes, namely, in $q^* \rightarrow q\gamma$ [5], $q^* \rightarrow qW$ [5], and $q^* \rightarrow qg$ [4], respectively, and therefore with different systematics.

In conclusion, we have searched for a resonance produced by the fusion of a gluon and a quark in $p\bar{p}$ collisions at a center of mass energy of 1.96 TeV which decays into a Z boson and a quark in the $Z \rightarrow e^+e^-$ decay channel. In the absence of a signal, we have determined 95% C.L. upper limits on the cross section times branching fraction as a function of the mass and width of the resonance. The present study is complementary to earlier searches because it has sensitivity to hypothetical models with enhanced couplings to the Z boson.

We thank the staffs at Fermilab and collaborating institutions, and acknowledge support from the DOE and NSF (USA); CEA and CNRS/IN2P3 (France); FASI, Rosatom and RFBR (Russia); CAPES, CNPq, FAPERJ, FAPESP and FUNDUNESP (Brazil); DAE and DST (India); Colciencias (Colombia); CONACyT (Mexico); KRF and KOSEF (Korea); CONICET and UBACyT (Argentina); FOM (The Netherlands); PPARC (United Kingdom); MSMT (Czech Republic); CRC Program, CFI, NSERC and WestGrid Project (Canada); BMBF and DFG (Germany); SFI (Ireland); The Swedish Research Council (Sweden); Research Corporation; Alexander von Humboldt Foundation; and the Marie Curie Program.

V. M. ABAZOV *et al.*

PHYSICAL REVIEW D **74**, 011104(R) (2006)

- [1] U. Baur, M. Spira, and P. M. Zerwas, *Phys. Rev. D* **42**, 815 (1990). NLO corrections for this process have not yet been carried out. In general, they are expected to increase the cross section, but are not expected to exceed 50% for this type of process.
- [2] J. Alliti *et al.* (UA2 Collaboration), *Nucl. Phys.* **B400**, 3 (1993).
- [3] F. Abe *et al.* (CDF Collaboration), *Phys. Rev. D* **55**, R5263 (1997).
- [4] V. Abazov *et al.* (D0 Collaboration), *Phys. Rev. D* **69**, 111101(R) (2004).
- [5] F. Abe *et al.* (CDF Collaboration), *Phys. Rev. Lett.* **72**, 3004 (1994).
- [6] T. Sjöstrand *et al.*, *Comput. Phys. Commun.* **135**, 238 (2001).
- [7] V. Abazov *et al.* (D0 Collaboration), Fermilab Report No. Fermilab-Pub-05/341-E (to be published).
- [8] S. Abachi *et al.* (D0 Collaboration), *Nucl. Instrum. Methods Phys. Res. A* **338**, 185 (1994).
- [9] G. C. Blazey *et al.*, hep-ex/0005012.
- [10] H. L. Lai *et al.*, *Eur. Phys. J. C* **12**, 375 (2000).
- [11] M. L. Mangano, *et al.*, *J. High Energy Phys.* 07 (2003) 001; M. L. Mangano, M. Moretti, and R. Pittau, *Nucl. Phys.* **B632**, 343 (2002); **B539**, 215 (1999).
- [12] I. Bertram *et al.*, FERMILAB Report No. FERMILAB-TM-2104, 2000 (unpublished).